

Mass transfer to tubular electrodes: ECE process

Rajinder Pal Singh^a, Tejwant Singh^a, Jatinder Dutt^b and Atamjyot^b

^a Department of Mathematics and Statistics, Punjab Agricultural University, Ludhiana-141004, India

^b Department of Chemical Engineering and Technology, Punjab University, Chandigarh-160014, India

Received 24 January 2000

The mathematical model of mass transport for linear sweep voltammetry under hydrodynamic conditions at tubular electrodes has been studied for ECE processes in which an irreversible chemical reaction is coupled between two reversible charge transfer reactions. The resulting boundary value problem is converted into system of two integral equations, which is solved numerically. The effects of axial flow rate, scan rate, potential difference, variation of chemical reaction rate and the effect of the ratio of number of electrons (n_2/n_1) involved in two charge transfer reactions on CV-voltammograms are investigated and shown graphically.

KEY WORDS: mass transport, linear sweep voltammetry, hydrodynamic conditions, ECE process

1. Introduction

In our earlier reported work, we have developed mathematical treatment of mass transport involved in linear sweep voltammetry (LSV), under hydrodynamic conditions for EC and CE processes [19,20]. Lately many research workers have used successfully tubular/channel [15,16], double channel [8], and hemi-cylinder [10] electrode for analytical and experimental investigations in ECE processes under steady state conditions, for electrochemical techniques [1–7,9,11–14,17,18].

In the present investigations, the theory of LSV has been extended to the ECE mechanism in which an irreversible chemical reaction is coupled between two reversible charge transfers. The mathematical approach used in this work is essentially the same as reported earlier [19,20]. Using integral transform method, the boundary value problem defining the convective diffusion-charge transfer kinetic processes has been converted into a system of two integral equations which were solved numerically using Wagner's method [21].

Though the systems in which the reversible charge transfer involves the reduction process have been investigated but conversion to oxidation processes is obvious. The theoretical current-potential curves have been obtained solving the integral equations numerically and the effects of axial flow rate, scan rate, variation of chemical reaction rate and effect of potential difference on current-potential curves are shown in graphs.

The effect of ratio of number of electrons involved in two charge transfer reactions on peak and steady state currents has also been studied and results are shown graphically.

2. Formulation of the problem

The reaction process in which first order homogeneous irreversible chemical reaction was coupled between two reversible electrode charge transfers, referred to as the ECE mechanism, is generalized as



where k_f is forward chemical reaction rate constant.

The mathematical model representing the above process in which the reactants are flowing through a tubular electrode, laminary, is

$$\frac{\partial C_A}{\partial t} + v_a(r) \frac{\partial C_A}{\partial z} = D_A \left[\frac{\partial^2 C_A}{\partial r^2} + \frac{1}{r} \frac{\partial C_A}{\partial r} \right], \quad (2.4)$$

$$\frac{\partial C_B}{\partial t} + v_a(r) \frac{\partial C_B}{\partial z} = D_B \left[\frac{\partial^2 C_B}{\partial r^2} + \frac{1}{r} \frac{\partial C_B}{\partial r} \right] - k_f C_B, \quad (2.5)$$

$$\frac{\partial C_C}{\partial t} + v_a(r) \frac{\partial C_C}{\partial z} = D_C \left[\frac{\partial^2 C_C}{\partial r^2} + \frac{1}{r} \frac{\partial C_C}{\partial r} \right] + k_f C_B, \quad (2.6)$$

$$\frac{\partial C_D}{\partial t} + v_a(r) \frac{\partial C_D}{\partial z} = D_D \left[\frac{\partial^2 C_D}{\partial r^2} + \frac{1}{r} \frac{\partial C_D}{\partial r} \right] \quad (2.7)$$

subject to

$$t = 0, \quad 0 \leq r \leq a, \quad 0 \leq z \leq 1; \\ C_A = C_A^*, \quad (2.8)$$

$$C_B = C_C = C_D (\approx 0),$$

$$t > 0, \quad r = 0, \quad 0 \leq z \leq 1; \\ C_A \rightarrow C_A^*, \quad (2.9)$$

$$C_B = C_C = C_D \rightarrow 0,$$

$$t > 0, \quad r = a, \quad 0 \leq z \leq 1; \\ D_A \frac{\partial C_A}{\partial r} = -D_B \frac{\partial C_B}{\partial r} = -\frac{i_1(t)}{n_1 F A_r} = -f_A(t), \quad (2.10)$$

$$D_C \frac{\partial C_C}{\partial r} = -D_D \frac{\partial C_D}{\partial r} = -\frac{i_2(t)}{n_2 F A_r} = -f_C(t).$$

For reversible charge transfer reaction at the electrode surface, the boundary condition is governed by Nernst equation:

$$\begin{aligned} t > 0, \quad r = a, \quad 0 \leq z \leq 1; \\ \frac{C_A}{C_B} &= \exp\left[\frac{n_1 F}{RT}(E(t) - E_{AB}^0)\right], \\ \frac{C_C}{C_D} &= \exp\left[\frac{n_2 F}{RT}(E(t) - E_{CD}^0)\right] \end{aligned} \quad (2.11)$$

and

$$E = E_i - vt, \quad (2.12)$$

where E_i is the initial electrode potential, v is the potential scan rate.

For further analysis, the diffusion coefficients

$$D_A = D_B = D_C = D_D = D \quad (2.13)$$

which leads to a well-known consequence that

$$C_A(r, z, t) + C_B(r, z, t) + C_C(r, z, t) + C_D(r, z, t) = C_A^*. \quad (2.14)$$

The significance of various variables and parameters is given in appendix.

3. Solution

Equations (2.4)–(2.7) are decoupled by using the transformations

$$\Psi = \frac{C_B + C_C}{C_A^*}, \quad (3.1)$$

$$\Phi = \frac{C_B}{C_A^*} \exp(k_f t), \quad (3.2)$$

and using the same set of non-dimensional variables and parameters as in [20], the model is transformed to a set of integral equations. For brevity, the assumptions and solution procedure are not repeated here and one can refer to our earlier work [19,20]. The set of integral equations involving concentrations C_A , C_B , C_C and C_D can be obtained using the transformations (3.1) and (3.2) are respectively

$$C_A = C_A^* - \frac{1}{\Lambda \sqrt{k_f D}} \int_0^{t'} f_A(\tau) g(\xi, t' - \tau) d\tau, \quad (3.3)$$

$$C_B = \frac{1}{\Lambda \sqrt{k_f D}} \int_0^{t'} f_A(\tau) g(\xi, t' - \tau) e^{-\Lambda^{-2}(t' - \tau)} d\tau, \quad (3.4)$$

$$C_C = \frac{1}{\Lambda \sqrt{k_f D}} \left[\int_0^{t'} f_A(\tau) g(\xi, t' - \tau) (1 - e^{-\Lambda^{-2}(t' - \tau)}) - \int_0^{t'} f_C(\tau) g(\xi, t' - \tau) \right] d\tau, \quad (3.5)$$

$$C_D = \frac{1}{\Lambda \sqrt{k_f D}} \int_0^{t'} f_C(\tau) g(\xi, t' - \tau) d\tau. \quad (3.6)$$

Since it is of interest to depict the behavior of current function $f(t')$ with respect to the known behavior of potential function $E(t')$. Substituting the expressions for C_A , C_B , C_C and C_D from equations (3.3)–(3.6) into the equation (2.11), we get the following integral equations, which are solved using Wagner method.

$$e^{(u_1 - y)} \int_0^y \chi(z) K_2(y - z) dz = 1 - \int_0^y \chi(z) K_1(y - z) dz, \quad (3.7)$$

$$\begin{aligned} & \int_0^y Q(z) K_1(y - z) dz + e^{u_2 - y\gamma} \int_0^y Q(z) K_1(y - z) dz \\ & = \int_0^y \chi(z) K_1(y - z) dz - \int_0^y \chi(z) K_2(y - z) dz, \end{aligned} \quad (3.8)$$

where

$$\sigma = \frac{n_1 F v}{RT P^2}; \quad y = \sigma t'; \quad z = \sigma \tau, \quad (3.9)$$

$$\delta = \Lambda^{-2} \sigma^{-1} = \frac{k_f RT}{n_1 F v}, \quad (3.10)$$

$$u_1 = \ln \theta_{AB} = \frac{n_1 F}{RT} (E_i - E_{AB}^0), \quad (3.11)$$

$$u_2 = u_1 \gamma = \ln \theta_{CD} = \frac{n_2 F}{RT} (E_i - E_{CD}^0), \quad (3.12)$$

$$K_1(y - z) = \sum_{n=1}^{\infty} \frac{1}{\lambda_n} \exp\left[-\frac{\lambda_n}{\sigma}(y - z)\right], \quad (3.13)$$

$$K_2(y - z) = \sum_{n=1}^{\infty} \frac{1}{\lambda_n} \exp\left[-\left(\frac{\lambda_n}{\sigma} + \delta\right)(y - z)\right], \quad (3.14)$$

$$\chi(z) = \frac{f_A(z)}{\sqrt{k_f D} \Lambda C_A^* \sigma}, \quad (3.15)$$

$$Q(z) = \frac{f_C(z)}{\sqrt{k_f D} \Lambda C_A^* \sigma}. \quad (3.16)$$

4. Result and discussion

The current functions $i_1(t')$ and $i_2(t')$ are related to the reductions of substances A and C by

$$i_1(t') = n_1 F A_r \Lambda \sqrt{k_f D} \sigma C_A^* \chi(\sigma t'), \quad (4.1)$$

$$i_2(t') = n_2 F A_r \Lambda \sqrt{k_f D} \sigma C_A^* Q(\sigma t') \quad (4.2)$$

and the total current and potential is given by

$$i(t') = n_1 F A_r \Lambda \sqrt{k_f D} \sigma C_A^* [\chi(\sigma t') + \gamma Q(\sigma t')], \quad (4.3)$$

$$E(t') - E_{AB}^0 = \frac{RT}{n_1 F} (u_1 - \sigma t'), \quad (4.4)$$

$$E(t') - E_{CD}^0 = \frac{RT}{n_2 F} (u_2 - \sigma t'). \quad (4.5)$$

The integral equation (3.7) involving only $\chi(\sigma t')$ as an unknown function has been solved independently and these values of $\chi(\sigma t')$ so obtained have been used in integral equation (3.8) to obtain values of $Q(\sigma t')$.

The effects of variation of scan rate and axial velocity on the voltammograms are depicted in figures 1 and 2, respectively. These effects are of similar and comparable in nature with our earlier reported work [20]. The effect of sharpness of peak currents or the repression of waves is on both the waves simultaneously.

The voltammograms exhibit either one or two waves. The exact form of the voltammogram depends on the separation of the waves, which enters in the calculations through the terms E_{AB}^0 and E_{CD}^0 . Equation (4.1) indicates that the current of substance A is independent of substance C so by considering the currents of the two reactants separately and taking the total current as the sum of the two currents, a clearer insight to the behavior of

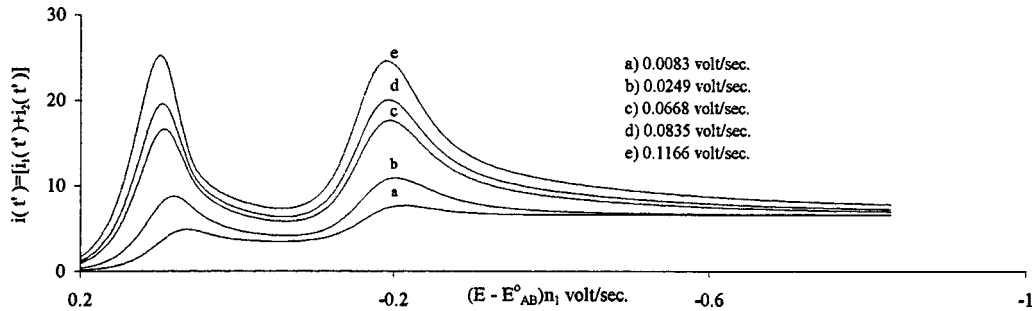


Figure 1. Variation of scan rate ($v_a = 0.5305$ cm/s, $\Delta E^0 = -0.18$ V/s, $\delta = 70$, $n_2 = n_1 = 1$).

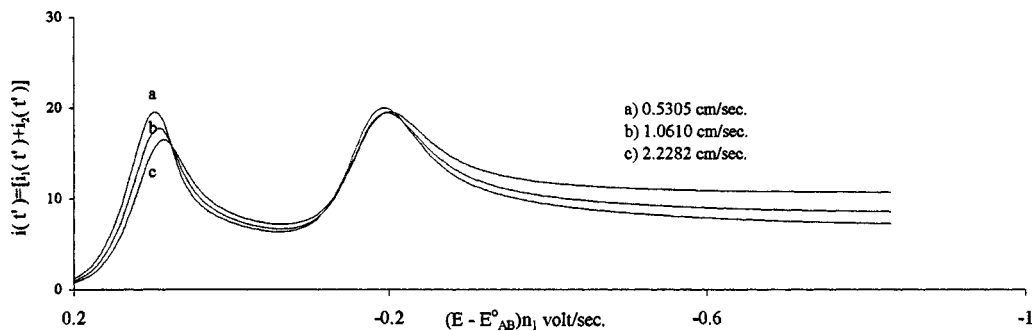


Figure 2. Variation of axial velocity ($v = 0.0835$ V/s, $\Delta E^0 = -0.18$ V/s, $\delta = 70$, $n_2 = n_1 = 1$).

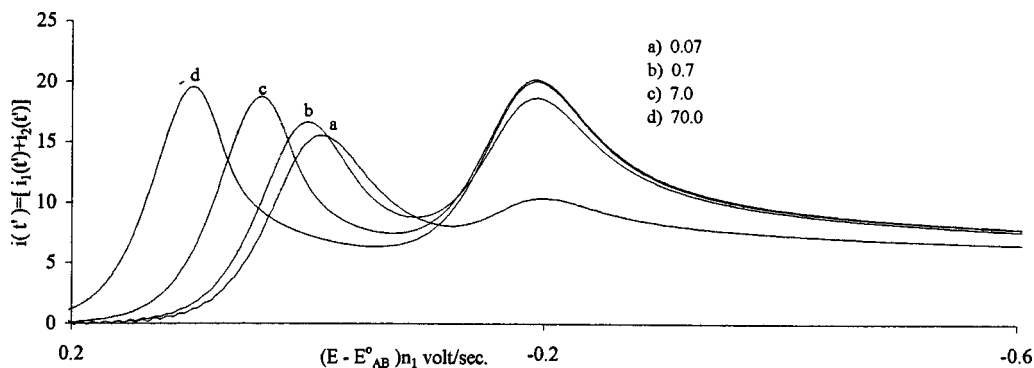


Figure 3. Variation of $\delta = RTk_f/n_1Fv$ ($v_a = 0.5305$ cm/s, $v = 0.0835$ V/s, $\Delta E_0 = -0.18$ V/s, $n_2 = n_1 = 1$).

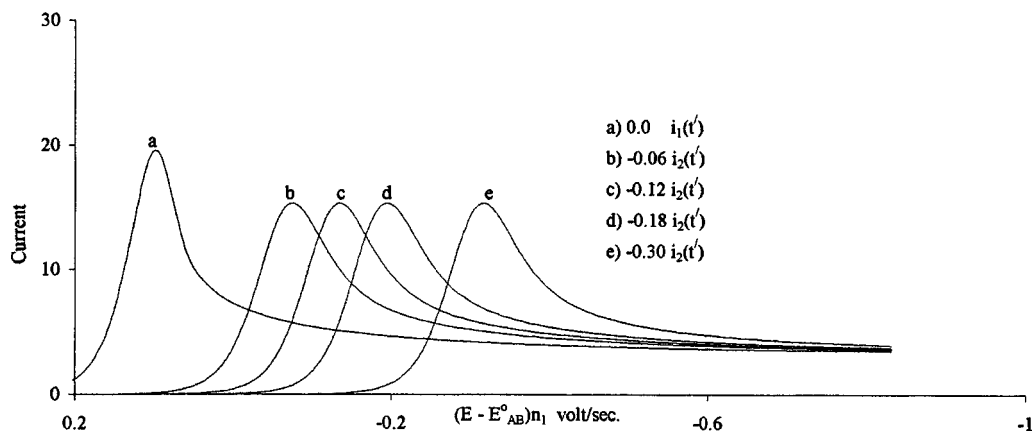


Figure 4. Effect of potential difference ($v_a = 0.5305$ cm/s, $v = 0.0835$ V/s, $\delta = 70$, $n_2 = n_1 = 1$).

the system can be obtained. For the first wave, the current corresponds to the reduction of substance A and the second wave reduction of C.

As the rate constants of different chemical reactions vary in magnitude, the effect of variation of the non-dimensional parameter $\delta = (k_f RT/n_1 F v)$ on the peak current is studied and the results are shown in figure 3. The second wave is strongly affected by variation in the kinetic parameter δ . With the increase in δ , a broad second wave appears which is spread over a relatively wide potential range. The peak current of first wave as well as the difference of peak potentials of both the waves increase with the increase in δ . The ratio of peak currents of the waves can be used to determine the rate of the chemical reaction. The second peak is measured to the base line determined by the extension of the first wave. Two additional factors namely the ratio n_2/n_1 and standard electrode potential difference $\Delta E^0 = E_{CD}^0 - E_{AB}^0$ also contribute to the shape of voltammograms. The wave separation of the second wave depends on the magnitude of ΔE^0 . The general shape of the function $i_2(t')$ is essentially constant for a particular

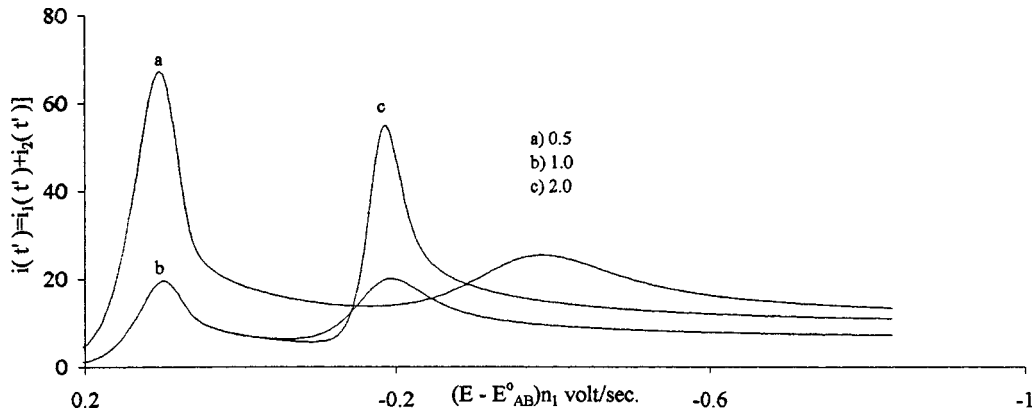


Figure 5. Effect of ratio of electrons (n_2/n_1) ($v_a = 0.5305$ cm/s, $v = 0.0835$ V/s, $\Delta E^0 = -0.18$ V/s, $\delta = 70$).

value of δ but the separation from first wave increases with the increase in the magnitude of ΔE^0 . The separation of waves is caused by the continued production of substance C during the scan and thus the concentration of the reactant at the electrode surface does not decrease rapidly as magnitude of ΔE^0 increases.

The number of electrons involved in two charge transfers enters into calculation in two ways. The first way how the functions $\chi(\sigma t')$ and $Q(\sigma t')$ are defined in equations (4.1) and (4.2), while the second arises when the kinetics interact with the Nernst equation. The current for the first wave is proportional to n_1^2 and the second wave is proportional to n_2^2 . So the peaks become sharper as n_1 and n_2 increases. The second effect appears when comparing $i_2(t')$ values for different values of the ratio n_2/n_1 . In addition to the change in peak height which is observed if the ratio n_2/n_1 varies, the relative sharpness of the peaks also changes which is shown in figure 5.

Appendix: Nomenclature

The values of various constants and parameters used for numerical calculations are given as follows:

a	radius of the electrode (0.1 cm),
l	length of the electrode (1.0 cm),
C_A^*	initial bulk molar concentration (10^{-7} mol ml $^{-1}$),
D	diffusion coefficient ($0.567 \cdot 10^{-5}$ cm s $^{-1}$),
R	gas constant (8.31 J mol $^{-1}$ K $^{-1}$),
T	absolute temperature (298 K),
F	Faraday's constant (96 487 cal mol $^{-1}$),
E^0	standard electrode potential (-0.063 V vs. SCE),
u_1	parameter ($= \ln \theta_{AB}$) representing the difference of initial potential E_i and standard electrode potential E_{AB}^0 (8),

u_2	parameter ($= \ln \theta_{CD}$) representing the difference of initial potential E_i and standard electrode potential E_{CD}^0 (8),
v	potential scan rate (0.5, 1.5, 4, 5, 7 V min ⁻¹),
v_a	axial flow velocity (0.5305, 1.0161, 2.2822 cm s ⁻¹),
σ	$nFv/RT P^2$, non-dimensional parameter,
n_1, n_2	number of electrons involved in charge transfer reactions (1),
k_f	forward chemical reaction rate (44.9 s ⁻¹),
δ	$(k_f)/(nFv/RT P^2)$, a non-dimensional kinetic parameter,
λ_n	magnitude of n th zero of $A'_i(\eta)$ (values of first seventy zeros of $A'_i(\eta)$ are used for calculations),
A_T	accessible surface area of the electrode ($= \pi a^2 l$).

References

- [1] L. Nadjo and J.M. Saveant, *J. Electroanal. Chem.* 48 (1973) 113.
- [2] E. Laviron and A. Vallat, *J. Electroanal. Chem.* 74 (1976) 297.
- [3] C. Amatore and J.M. Saveant, *J. Electroanal. Chem.* 85 (1977) 27.
- [4] R.G. Compton, M.B.G. Pilkington, G.M. Stearn and P.R. Unwin, *J. Electroanal. Chem.* 238 (1987) 43.
- [5] J. Galvez, J. Zapata and A. Molina, *J. Electroanal. Chem.* 219 (1987) 1.
- [6] J. Galvez and S.M. Park, *J. Electroanal. Chem.* 259 (1989) 21.
- [7] A. Neudeck and J. Dittrich, *J. Electroanal. Chem.* 264 (1989) 91.
- [8] P.R. Unwin, *J. Electroanal. Chem.* 297 (1991) 103.
- [9] K. Scott and A.N. Haines, *J. Appl. Electrochem.* 24 (1994) 703.
- [10] J.A. Alden, R.G. Compton and R.A.W. Dryfe, *J. Electroanal. Chem.* 397 (1995) 11.
- [11] I. Cserevenyak, G.H. Kelsall and W. Wang, *Electrochim. Acta* 41 (1996) 573.
- [12] A.K. Kontturi, K. Kontturi, L. Murtomaki and D.J. Schiffrin, *J. Electroanal. Chem.* 418 (1996) 131.
- [13] M.L. Alcaraz, A. Molina and M.L. Tenes, *Electrochim. Acta* 42 (1997) 1351.
- [14] P. Simon and G. Farsang, *J. Electroanal. Chem.* 432 (1997) 117.
- [15] J.A. Alden and R.G. Compton, *J. Phys. Chem.* 101 (1997) 9741.
- [16] J.A. Alden and R.G. Compton, *J. Electroanal. Chem.* 415 (1996) 1.
- [17] W.J. Aixill, J.A. Alden, F. Prieto, G.A. Wallis, R.G. Compton and M. Rueda, *J. Phys. Chem.* 102 (1998) 1515.
- [18] P.J. Mahon and K.B. Oldham, *J. Electroanal. Chem.* 445 (1998) 179.
- [19] T. Singh, R.P. Singh and J. Dutt, *J. Math. Chem.* 17 (1995) 335.
- [20] T. Singh, R.P. Singh and J. Dutt, *J. Math. Chem.* 23 (1998) 297.
- [21] C. Wagner, *J. Math. Phys.* 32 (1954) 289.